



A simple synthesis of nitrate cancrinite from natural bentonite

Sung Man Seo¹ · Daniel Kim¹ · Daeyoung Kim^{1,2} · Jae-Hwan Kim¹ · Ye Ji Lee¹ · Ki-Min Roh^{1,2} · Il-Mo Kang¹

Published online: 19 January 2018

© Springer Science+Business Media, LLC, part of Springer Nature 2018

Abstract

A nearly pure, pale brown, spherical, nitrate cancrinite zeolite was successfully synthesized from natural bentonite as starting material with acidic activation treatment via hydrothermal method at 368 K for 24 h. The effect of different NaOH concentrations (pH at around 12) was investigated without addition of silica and aluminum sources. The effect of different NaOH concentrations (pH at around 12) was investigated without addition of silica and aluminum sources. The final products were characterized by powder X-ray diffraction, scanning electron microscopy, elemental and thermal analyses, infrared (IR) spectroscopy, and Brunauer–Emmett–Teller (BET) surface area measurements. While the Si/Al ratio of ideal cancrinite is 1.0, the Si/Al ratio of the product framework is approximately 1.76, apart from trace components. Unique single nitrate band was observed in both IR and thermogravimetric measurements, indicating that pure cancrinite was synthesized. This study showed that pure nitrate cancrinite was obtained with NaOH concentrations from 8 to 12 M, independent of NaOH contents on crystallization. Through this study, we proposed a simple synthesis method for pure nitrate cancrinite from bentonite for the purpose of recycling natural clay minerals.

Keywords Nitrate cancrinite · Synthesis · Hydrothermal method · Bentonite · NaOH

1 Introduction

Zeolites are microporous crystalline aluminosilicates with well-defined open frameworks based on an infinitely extending three dimensional network of silicon and aluminum tetrahedra linked to each other with shared oxygen atoms [1]. Due to their unique structural properties, these porous materials are widely used as ion-exchangers, catalysts, and

adsorbents. Although zeolites can be obtained from natural deposits, these materials are generally synthesized from sodium aluminosilicate gel by hydrothermal method to find novel materials, using commercial reagents. Otherwise, natural clay minerals are also used as starting materials for zeolite synthesis because of their low costs [2–5].

Cancrinites (framework type code CAN) are one of the feldspathoid group of minerals, but they can also be regarded as zeolite due to their porous aluminosilicate framework structures with a chemical formula $[\text{Na}_6^+ \text{Ca}^{2+} \text{CO}_3^{2-} (\text{H}_2\text{O})_2] [\text{Si}_6 \text{Al}_6 \text{O}_{24}] \text{-CAN}$ [1, 6, 7]. Their framework consists of parallel 6-rings stacking along the c-axis in an AB–AB sequence in the hexagonal symmetry $P6_3$ [6–15]. Thus, this arrangement of sheets gives large 12-ring channels parallel to the 6_3 axis and chains of smaller 11-hedral cages (ϵ -cages) along the threefold axes [6–15]. While the small cage contains non-framework cations and water molecules, the large channel is filled with exchangeable cations and intracrystalline anions such as carbonate in natural form [6–15].

Since the first report on crystallization experiments by Eitel [16], cancrinites have been extensively synthesized with a variety of anion species such as carbonate [17–24], nitrate [6, 25–28], hydroxide [12, 18, 29], and others [25,

Sung Man Seo and Daniel Kim have contributed equally to this work.

Electronic supplementary material The online version of this article (<https://doi.org/10.1007/s10934-018-0569-4>) contains supplementary material, which is available to authorized users.

✉ Sung Man Seo
smseo@kigam.re.kr

✉ Ki-Min Roh
kmroh@kigam.re.kr

¹ Advanced Geo-materials R&D Department, Pohang Branch, Korea Institute of Geoscience and Mineral Resources, Pohang 37559, South Korea

² Department of Nanomaterials Science and Engineering, University of Science and Technology, Daejeon 34113, South Korea

26, 30, 31] and were characterized by various techniques. In an optimization study where hydrothermal formation of nitrate cancrinite under varying reaction conditions of Si/Al ratio from 0.5 to 3.0 at 473 K and autogenous pressure and at 773 K and 0.15 GPa, the optimal Si/Al ratio is suggested to be 1.2 of the starting materials using zeolite X and a mixture of sodium silicate and sodium aluminate [6]. The thermal stability of carbonate cancrinite prepared in the system $\text{Na}_2\text{O}-\text{CaO}-\text{Al}_2\text{O}_3-\text{SiO}_2-\text{CO}_2-\text{H}_2\text{O}$ at 2 kbar and in the presence of a mixed $\text{H}_2\text{O}-\text{CO}_2$ fluid was studied to demonstrate that water plays important role [14]. In the study of synthesis of carbonate cancrinite in the system $\text{Na}_2\text{O}-\text{SiO}_2-\text{Al}_2\text{O}_3-\text{Na}_2\text{CO}_3-\text{H}_2\text{O}$ under hydrothermal reactions at 353 and 473 K, it was indicated that cancrinite crystallization reacted extremely sensitively on the temperature within the reaction vessel, while concentration and alkalinity of the reactant were not important factors for phase formation [15]. The pure nitrate cancrinite has been synthesized using mixed solution of sodium silicate, sodium aluminate, sodium nitrate, and sodium hydroxide in neutral pH at 363 K and determined the formation enthalpy from the constituent oxides and elements [27]. Recently, the formation conditions of nitrate cancrinite and chlorosodalite zeolites were investigated by the influence of pH and $\text{NO}_3^-/\text{Cl}^-$ anionic composition on the synthesis of the cancrinite–sodalite system [28].

Bentonite is a clay mineral mostly composed of montmorillonite, which has been extensively studied for its pharmaceutical and cosmetic applications due to their high adsorption ability, high specific surface area, high cation exchange capacity, interlayer reactions, and chemical inertness [32–39]. Prior to its applications, purification processes to select montmorillonite from bentonite are required. After purification, residual bentonite can be recycled through chemical reaction such as hydrothermal method. In present study, we report that pure nitrate cancrinite was successfully synthesized using natural Ca-type bentonite as starting material in the presence of sodium hydroxide at low temperature. The synthesized material was subjected to phase identification and compositional analyses in search for purposes of finding its applications.

2 Experimental section

2.1 Synthesis

Natural bentonite was obtained from Gampo40 (BGP40) in Korea and was used in synthesis without further purification. The chemical compositions of bentonite used as starting material are shown in Table 1. The 3 g of bentonite powder meshed through a #18 sieve was firstly reacted with 20 mL of aqua regia (3:1 (v/v) concentrated HCl (ACS reagent, 37%, Sigma-Aldrich): HNO_3 [ACS reagent, 70%, Sigma-Aldrich]) in the 125-mL polypropylene (PP) bottle at room temperature for 4 h. Then, 50 mL NaOH (Sigma-Aldrich) solution with various concentration (6, 8, 10, and 12 M) was slowly added to the treated bentonite mixture in each 125-mL PP bottle, followed by vigorous stirring at room temperature for 4 h. After reaction, the final pH of the solutions were 12.7, 12.7, 12.5, and 12.4, respectively. The bottle containing the final mixture was placed in a convection oven at 368 K for 24 h. The products were filtered and washed with distilled water 10 times, and dried at 333 K for 2 days prior to characterization.

2.2 Analytical methods

The reaction product was characterized by powder X-ray diffraction (XRD), scanning electron microscopy (SEM), X-ray fluorescence (XRF), Fourier transform IR (FT-IR), and thermogravimetric (TG) analysis. Powder XRD patterns were recorded on a Rigaku MiniFlex 600 diffractometer with $\text{Cu K}\alpha$ radiation ($\lambda = 1.5406 \text{ \AA}$) at 40 kV and 15 mA. Data were collected over the 2θ range of $2^\circ-70^\circ$ with a step size of 0.02° . Indexing of the obtained XRD patterns was carried out using the Crystallographica Search-Match (CSM) software (Oxford Cryosystems, Oxford, UK). Crystal morphology and average size were examined using ZEISS environmental scanning electron microscopy (ESEM, Model EVO LS25), operating at 10 kV. The chemical compositions of the samples were determined by energy dispersive X-ray fluorescence spectrometer (Rigaku NEX CG). The FT-IR spectra were recorded on Thermo Nicolet iN 10 FT-IR Microscope. TG analysis was carried out using Setaram Labsys Evo thermal analyzer in flowing N_2 gas with a heating rate of 10 K/min in the range from room temperature to 1373 K.

Table 1 Chemical compositions of natural bentonite and as-made cancrinite

Material	Weight (%)							Total
	SiO_2	Al_2O_3	Na_2O	MgO	CaO	Fe_2O_3	LOI ^a	
Natural bentonite	52.77	13.53	1.15	4.62	1.62	2.81	23.5	100.0
As-made cancrinite	35.83	17.29	14.36	6.26	2.73	4.22	19.3	100.0

^aLoss on ignition

The BET surface area was detected by Quantachrome Instruments Quadrasorb-EVO at 77 K.

3 Results and discussion

The chemical composition of the natural bentonite obtained by EDXRF analysis, given in Table 1, indicates that silica and alumina were major component and calcium and sodium were non-framework cations, along with trace elements of magnesium and iron oxides. As shown in Fig. 1, the powder XRD patterns showed that the natural bentonite was consisted mainly of montmorillonite with minor amounts of albite, quartz, and opal-CT. After acidic activation treatment, these minerals that organized bentonite were dissolved in aqua regia. Indeed, it was confirmed that the XRD patterns of reaction product without adding NaOH solution crystallized at 368 K for 24 h showed amorphous materials with a little sediment of heulandite as natural zeolite, quartz, and opal-CT (see the Supporting Information Figure S1).

Figure 1 shows the powder XRD pattern of as-made cancrinite obtained after hydrothermal synthesis with adding 10 M NaOH solution. Four strong X-ray peaks around $2\theta = 13.9^\circ$, 18.8° , 24.2° , and 27.4° respective to the (110), (101), (300), and (211) reflections of the CAN structure [6, 7] revealed the corresponding material. Thus, unit cell parameters for the as-made cancrinite were determined by PDXL software [40]. The calculated parameters are $a = 12.661(2) \text{ \AA}$ and $c = 5.1853(10) \text{ \AA}$, which are in agreement with previously reported values of $a = 12.668(2) \text{ \AA}$ and $c = 5.166(1) \text{ \AA}$ for nitrate cancrinite determined by single-crystal X-ray technique [6] and $a = 12.6802(7) \text{ \AA}$ and $c = 5.1872(3) \text{ \AA}$ for nitrate cancrinite determined by Rietveld analysis [27], respectively. The chemical composition

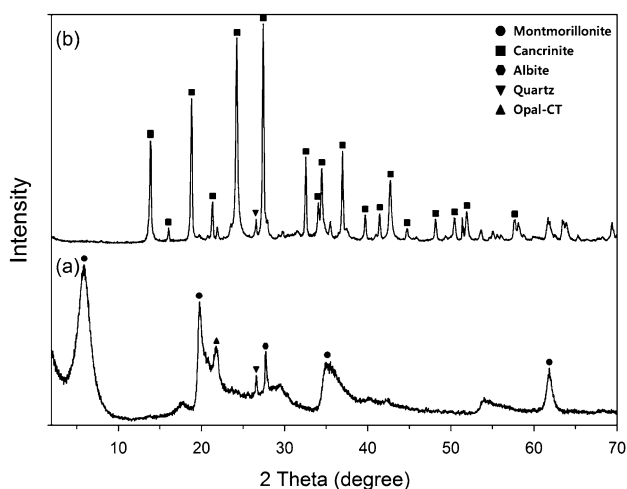


Fig. 1 X-ray diffraction patterns of (a) natural bentonite and (b) as-made cancrinite

of as-made cancrinite determined by EDXRF analysis (Table 1) showed that the framework Si/Al ratio was 1.76. This is higher than the ideal ratio of cancrinite framework composed of Si and Al atoms, which is Si/Al = 1.0. It is assumed that Si/Al ratio of natural bentonite was too high (Si/Al = 3.3) as starting material for hydrothermal synthesis. In previous reports of zeolite synthesis, sodium aluminate or aluminum hydroxide as additional alumina source was supplemented prior to hydrothermal synthesis in order to compensate the high Si/Al ratio of bentonite [2–4]. It is uncertain that trace components of magnesium and iron participated in cancrinite crystallization to the zeolite framework, or these acted as exchangeable cations, along with Na^+ and Ca^{2+} ions.

For comparison, effect of NaOH for cancrinite crystallization was examined using various NaOH concentrations (6, 8, 10, and 12 M) in the reaction mixture. All synthetic products were obtained as pale brown powder. As shown in Figs. S1–S5 of the Supporting Information, cancrinite is major product, but quartz as impurity is remained in all samples; it seemed that not all quartz was dissolved in aqua regia. There was no significant difference in phase formation among the four samples with varying concentrations of NaOH of the hydrothermal solution. This result is in agreement with results on synthesis of carbonate cancrinite prepared by lower reaction temperature with alkalinities of 12 M and higher [15].

The crystal habit of cancrinite typically appears in spherical, prismatic, hexagonal prism, needle, fractal shape, etc. Figure 2 shows that as-made cancrinite had a spherical particle shape and approximate average particle sizes of 15–20 μm , clearly indicating nearly pure nitrate cancrinite synthesized. This result is strongly supported by the FT-IR spectra of as-made cancrinite material (Fig. 3). The absorption bands of cancrinite framework related with typical symmetric T–O–T vibrations at 469, 578, 617, and 699 cm^{-1} and asymmetric T–O–T vibrations at 956 and 1118 cm^{-1} were clearly observed [6, 15, 41]. The bending mode at 1650 cm^{-1} and the broad band between 3100 and 3700 cm^{-1} were found due to O–H stretch of water molecules. The prominent single band was found at 1423 cm^{-1} which is due to the nitrate ion, NO_3^- , bending as non-framework anion. In the bending mode, additionally, two bands around at 2360 cm^{-1} correspond to the atmospheric CO_2 due to ATR-IR measurement. After calcination at 1373 K, the band at 1423 cm^{-1} disappeared, but two bands at around 2360 cm^{-1} remained. In previous reports, vibrations at 1410 and 1455 cm^{-1} [15] and at 1425 cm^{-1} [27] were assigned to carbonate and nitrate, respectively, inside the framework. As pointed out in systematic study of the IR spectra of cancrinite of ideal composition, disordered cancrinite, intermediate phase between cancrinite and sodalite, and basic sodalite [6, 15, 27], phase analysis

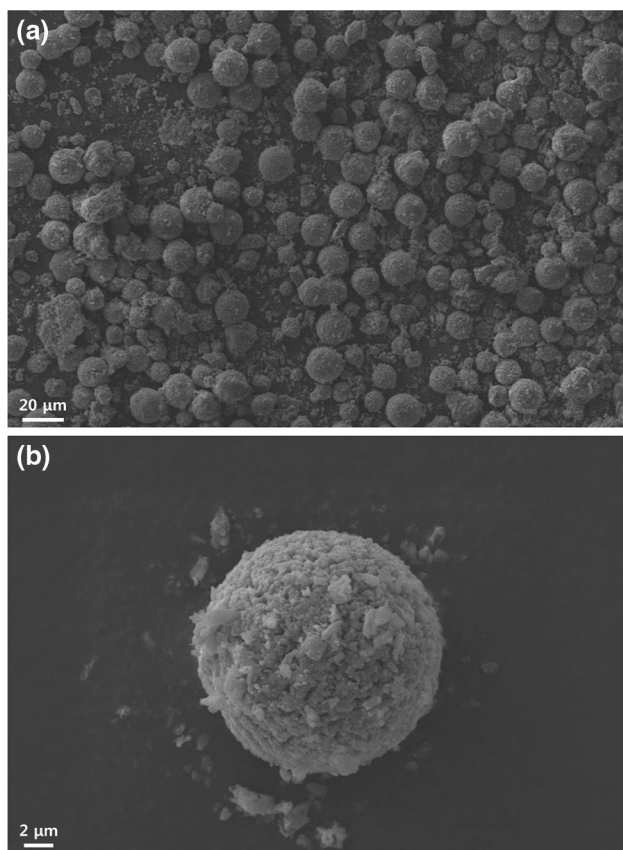


Fig. 2 SEM images of as-made cancrinite magnified at (a) $\times 1000$ and (b) $\times 7000$

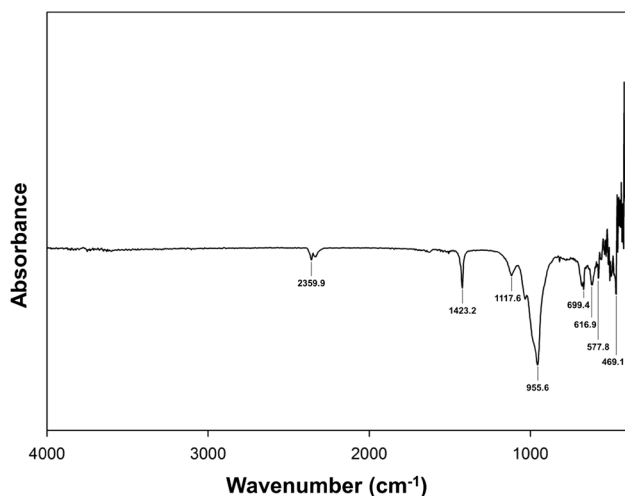


Fig. 3 FT-IR spectrum of as-made cancrinite

of synthetic cancrinite and cocrystallization impurities such as mainly sodalite and nepheline can be identified by comparing the IR spectra according to the corresponding absorption bands of the zeolite framework.

The results of thermogravimetry of as-made cancrinite synthesized in this study are in agreement with previously reported TG studies [6, 14, 15, 21, 42]. Through two strong exothermic peaks at 483 K for external water molecules and at 591 K for internal water, the first dehydration was completed at about 673 K (Fig. 4). When further heated up to 1373 K, the remarkable endothermic peak at 1071 K appeared. This indicated crystallinity destruction of the zeolite framework related to the decomposition of the enclathrated sodium nitrate according to the reaction $2\text{NaNO}_3 \rightarrow \text{Na}_2\text{O} + \text{N}_2 + 2.5\text{O}_2$, similar to the result observed in the case of nitrate cancrinite [27] and carbonate cancrinite [15].

While the natural bentonite had a BET surface area of $105 \text{ m}^2/\text{g}$ with a micropore volume of 0.046 mL/g , as-made cancrinite synthesized in this study showed a BET surface area of $51 \text{ m}^2/\text{g}$ with a micropore volume of 0.018 mL/g , which are smaller than the starting natural bentonite. This is due to the phase transition from aluminum phyllosilicate structure to aluminosilicate framework. According to the results from previous studies [42–45], the BET surface area of a pure cancrinite material was close to $10 \text{ m}^2/\text{g}$.

On the basis of characterization results of as-made cancrinite synthesized in this study, this zeolite has not led to technical and industrial applications because of mainly stacking disorder resulting in blocked channels and pores in the framework structure, cocrystallization impurities such as mainly sodalite, and insufficient studies on searching further application [15, 25]. For finding its application, we carried out to measure CO_2 adsorption isotherm at 298 K on as-made cancrinite (see the Supporting Information Fig. S6); CO_2 uptake is below 0.5 mmol/g at pressure 1 bar. Due to these reasons, we suggest that this material can be used in cosmetic application that replacement of plastic particles in scrub-related products due to its spherical shape,

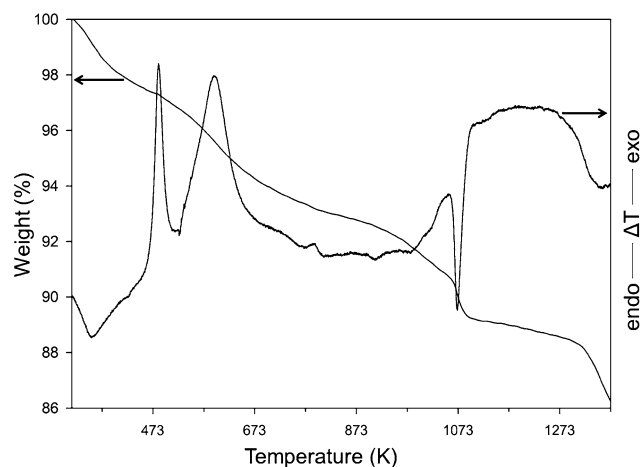


Fig. 4 TG-DTA curves of as-made cancrinite

uniform size of *ca.* 15–20 μm , and high cation-exchange property with low Si/Al ratio for external and/or internal modifications.

4 Conclusion

A simple synthesis procedure for pure nitrate cancrinite zeolite using natural bentonite as starting material with acidic treatment has been proposed. The product had a high crystallinity and thermal stability with a very uniform crystal sizes, ranging from 15 to 20 μm . As-made cancrinite without sodalite formation as impurity is crystallized in a wide range of NaOH concentrations in the synthesis mixture. The results presented a considerable contribution to the synthesis study of special material which has its potential importance in industrial applications.

Acknowledgements This research was supported by the Basic Research Project (Grant 18-3214) of the Korea Institute of Geoscience and Mineral Resources (KIGAM) funded by the Ministry of Science, ICT, and Future Planning of Korea.

References

1. D.W. Breck, *Zeolite Molecular Sieves*. (Wiley, New York, 1974)
2. A. Chaisena, K. Rangsrivatananon, *Mater. Lett.* **59**, 1474–1479 (2005)
3. H. Faghihian, N. Godazandeha, *J. Porous Mater.* **16**, 331–335 (2009)
4. H. Ma, Q. Yao, Y. Fu, C. Ma, X. Dong, *Ind. Eng. Chem. Res.* **49**, 454–458 (2010)
5. C. Chen, D.-W. Park, W.-S. Ahn, *Appl. Surf. Sci.* **292**, 63–37 (2014)
6. J.-Ch Buhl, F. Stief, M. Fechtelkord, T.M. Gesing, U. Taphorn, C. Taake, *J. Alloys Compd.* **305**, 93–102 (2000)
7. C. Baerlocher, L. McCusker, Data of zeolite structures, <http://www.iza-structure.org/databases/>
8. G. Gossner, F. Mussgnug, *Z. Kristallogr.* **73**, 52–60 (1930)
9. O. Jarchow, *Fortschr. Miner.* **40**, 55–56 (1962)
10. O. Jarchow, *Z. Kristallogr.* **122**, 407–422 (1965)
11. H.D. Grundy, I. Hassan, *Can. Miner.* **20**, 239–251 (1982)
12. I. Hassan, H.D. Grundy, *Can. Miner.* **29**, 377–383 (1991)
13. I. Hassan, P.R. Buseck, *Can. Miner.* **30**, 49–59 (1992)
14. M. Sirbescu, D.M. Jenkins, *Am. Miner.* **84**, 1850–1860 (1999)
15. K. Hackbarth, Th..M. Gesing, M. Fechtelkord, F. Stief, J.-C. Buhl, *Microporous Mesoporous Mater.* **30**, 347–358 (1999)
16. W. Eitel, *Jb. Miner.* **II** 45–61 (1922)
17. A.D. Edgar, B.J. Burley, *Can. Miner.* **7**, 631–642 (1963)
18. A.D. Edgar, *Can. Miner.* **8**, 53–67 (1963)
19. Y.I. Smolin, Y.F. Shepelev, I.K. Butikova, I.B. Kobayakov, *Sov. Phys. Crystallogr.* **26**, 33–35 (1981)
20. A. Emiraliev, I.I. Yamzin, *Sov. Phys. Crystallogr.* **27**, 27–30 (1982)
21. J.-C. Buhl, *Thermochim. Acta.* **178**, 19–31 (1991)
22. G. Hermeler, J.-Ch Buhl, W. Hoffmann, *Catal. Today.* **8**, 415–426 (1991)
23. N. Bresciani-Pahor, M. Calligaris, G. Nandin, L. Randaccio, *Acta Cryst.* **B38**, 893–895 (1982)
24. R. Klaska, K.-H. Klaska, O. Jarchow, *Z. Kristallogr.* **149**, 135–137 (1979)
25. R.M. barrer, J.F. Cole, H. Villiger, *J. Chem. Soc. A.* 1523–1531 (1970)
26. F. Hund, *Z. Anorg. Allg. Chem.* **509**, 153–160 (1984)
27. Q. Liu, H. Xu, A. Navrotsky, *Microporous Mesoporous Mater.* **87**, 146–152 (2005)
28. F. Ocanto, R. Álvarez, C.U. de Navarro, A. Lieb, C.F. Linares, *Microporous Mesoporous Mater.* **116**, 318–322 (2008)
29. N. Bresciani Pahor, M. Calligaris, L. Randaccio, *Acta Crystallogr.* **B38**, 893–895 (1982)
30. K. Latham, C.D. Williams, C.V.A. Duke, *Zeolites.* **17**, 513–516 (1996)
31. G.-G. Lindner, K. Hoffmann, K. Witke, D. Reinen, C. Heinemann, W. Koch, *J. Solid State Chem.* **126**, 50–54 (1996)
32. E. Gamiz, J. Linares, R. Delgado, *Appl. Clay Sci.* **6**, 359–368 (1992)
33. R. Bolger, *Ind. Min.* 52–63 (1995)
34. F.H. Lin, Y.H. Lee, C.H. Jian, J.M. Wong, M.J. Shieh, C.Y. Wang, *Biomaterials.* **23**, 1981–1987 (2002)
35. M.I. Carretero, *Appl. Clay Sci.* **21**, 155–163 (2002)
36. A. López-Galindo, C. Viseras, P. Cerezo, *Appl. Clay Sci.* **36**, 51–63 (2007)
37. J.-H. Choy, S.-J. Choi, J.-M. Oh, T. Park, *Appl. Clay Sci.* **36**, 122–132 (2007)
38. A. Abdel-Motelib, Z.A. Kader, Y.A. Ragab, M. Mosalamy, *Appl. Clay Sci.* **52**, 140–144 (2011)
39. I. Valentina, M. Eleonora, S. Francesca, R. Marcello, B. Alessia, T. Eleonora, M. Paola, E. Leo, *Clays Clay Miner.* **64**(6), 719–731 (2016)
40. Advanced integrated, X-ray powder diffraction suite. *Rigaku J.* **28**(1), 29–30 (2012)
41. E.M. Flanigen, H. Kathami, H.A. Szymanski, *Adv. Chem. Ser. Mol Sieve Zeolites I* **101**, 201–229 (1971)
42. H. Shao, T.J. Pinnavaia, *Microporous Mesoporous Mater.* **133**, 10–17 (2010)
43. M.C. Barnes, J. Addai-Mensah, A.R. Gerson, *Colloid Surf. A* **157**, 101–116 (1999)
44. M.C. Barnes, J. Addai-Mensah, A.R. Gerson, *Microporous Mesoporous Mater.* **31**, 287–302 (1999)
45. C.F. Linares, S. Sánchez, C.U. de Navarro, K. Rodríguez, M.R. Goldwasser, *Microporous Mesoporous Mater.* **77**, 215–221 (2005)